
INDUSTRIAL CRYSTALLIZATION FROM SOLUTION: THE PRECIPITATION OF SODIUM PERBORATE[#]

Iztok Livk

CSIRO Minerals, PO Box 90, Bentley WA 6982, Australia

Ciril Pohar

Faculty of Chemistry and Chemical Technology, University of Ljubljana, Aškerčeva 5, 1000 Ljubljana, Slovenia

[#] This paper is dedicated to Professor Roman Modic on the occasion of his 90th birthday

Received 30-05-2001

Abstract

Methods used in the analysis of an industrial crystallization process are presented in this article. They are implemented in the development of a population balance based model for the sodium perborate precipitation. The precipitation kinetics such as nucleation, growth and agglomeration are estimated using a novel estimation procedure, which enables the determination of crystallization kinetics from the experimental crystal size distributions. The values obtained for the crystal growth rate agree well with the values determined by other authors.

Introduction

The aim of this article is to illustrate some of the important steps involved in the analysis of an industrial crystallization process. Our discussion, which is focused on the sodium perborate system, includes topics such as crystallisation modelling, simulation and kinetic parameter estimation. In addition to this, we also attempt to summarize our results on the precipitation of sodium perborate.

Crystallization from solution is considered to be one of the oldest separation techniques, where a solid phase is created from a liquid. The main advantage of crystallization is that it can produce high purity substances at low energy consumption. The application of this technique in the chemical industry ranges from the bulk production of basic materials, such as fertilizers and sugar, to the production of specialty chemicals and pharmaceuticals.

To induce and maintain crystallization from solution a driving force is required. It is usually referred to as supersaturation of the system. Different expressions are generally used to define the supersaturation. Commonly, an expression in the form of a

concentration difference is used

$$\Delta c = c - c^*,$$

where c is the solute concentration and c^* is the equilibrium concentration. The other frequently used expressions are the so-called supersaturation ratio

$$S = \frac{c}{c^*}$$

and the relative supersaturation

$$\sigma = \frac{c - c^*}{c^*}$$

In the case of the systems of highly soluble substances, the supersaturation can be created by evaporation or cooling. When the substances are only slightly soluble, the supersaturation is usually created by mixing the reactants. This type of crystallization is also called reactive crystallization or precipitation. Using this operation, sodium perborate tetrahydrate is produced by the reaction between sodium metaborate and hydrogen peroxide in an aqueous solution. The process has great industrial importance and was studied by a number of researchers. The solubility in this system has been studied for example in the work of Yüksel *et al.*,¹ Livk *et al.*² and Chianese *et al.*³ The quality of the solid product, however, is mainly determined by the relative magnitudes of the growth, nucleation and agglomeration kinetics. The growth of crystals has been studied by Söhnel *et al.*,⁴ Chianese *et al.*^{5,6} and Livk *et al.*⁷ Dugua and Simon,⁸ and Chianese *et al.*⁶ were the first to explore the nucleation rate in this system. In both studies, however, the nucleation rate was determined indirectly. In the work of David and Bossoutrot,⁹ the agglomeration process was also introduced into the sodium perborate precipitation model.

Model development

In the modelling of an industrial crystallization process, a description of the solid phase is usually of prime importance. Due to the interactions present in the crystallization process,¹⁰ the information on the solid phase is needed also in the case when only the yield of a crystallization process is of interest. The solid phase consists of

a population of crystals, which typically differ in size, shape and purity. A mathematical tool, which describes the transient of the distribution of a crystal population is known as population balance equation (PBE). Its use in the modelling of crystallization processes has been formalized by the work of Randolph and Larson.¹¹ In principle, a population balance describes how the crystal number distribution changes due to changes in the given coordinates and any crystal formation and removal mechanisms. The general PBE for an ideally stirred reactor is given as¹²

$$\frac{\partial(nV)}{\partial t} + V\nabla\left(\frac{\partial\mathbf{z}}{\partial t}n\right) = V(B - D) - \sum_k F_k n_k \quad (1)$$

where n is the population density function, n_k is the population density function of the k th stream, \mathbf{z} is the set of internal coordinates, B and D are the density functions of formation and removal of crystals, F_k is the volumetric flow rate of the k th stream, and V is the slurry volume. The set, \mathbf{z} , can include coordinates such as size, purity and shape. However, here we restrict our discussion only to the modelling of the crystal size distribution (CSD).

The development of the crystal size distribution depends on various kinetic processes such as nucleation, crystal growth and agglomeration. They can be incorporated into Eq.1 resulting in

$$\frac{\partial(Vn)}{\partial t} + V \frac{\partial(Gn)}{\partial L} = VB^o\delta(L - L_0) + V(B_a - D_a) - \sum_k F_k n_k \quad (2)$$

where n is the number density function defined as $1/V dN/dL$, G is linear crystal growth rate, L is the characteristic size of crystals, L_0 is the size of nucleus, B^o nucleation rate and $\delta(L-L_0)$ the Dirac delta function, and B_a and D_a are the birth and death rates due to agglomeration.

The solution of the above PBE is simplified with the introduction of discretized population balance,^{13,14} which for the i th size interval can be written as

$$\frac{d(VN_i)}{dt} + V[G(L_{i+1})n(L_{i+1}) - G(L_i)n(L_i)] = VB_{u,i} + VR_{a,i} \quad ; \quad i=1..m \quad (3)$$

where N_i is the number of crystals per slurry volume in the i th size interval, $n(L_i)$ is the number density at the border of the i th size interval, L_i is the crystal size at the border of the i th size interval, $B_{u,i}$ is the source rate, which is nonzero only for $i=1$, $R_{a,i}$ is the net formation of crystals in the i th size interval due to agglomeration, and m is the total number of size intervals. For the complete description of an isothermal crystallization process a mass balance is also required. The mass balance of the sodium perborate (NaPB) in solution can be written as

$$\frac{d(\varepsilon cV)}{dt} = c_{H_2O_2} F_{H_2O_2} \frac{M_{NaPB}}{M_{H_2O_2}} - 3\rho_s k_v V \int_{L_1}^{L_{m+1}} nL^2 G dL - \varepsilon VR_n(\bar{L}_1) \quad (4)$$

where the second and third term on the right hand side of the equation account for the mass transfer to the solid phase via formation and growth of crystals. In this case, H_2O_2 is the limiting component in solution. Accordingly, the solid phase mass balance is

$$\frac{dm_s}{dt} = 3\rho_s k_v V \int_{L_1}^{L_{m+1}} nL^2 G dL + \varepsilon VR_n(\bar{L}_1) \quad (5)$$

In Eqs. 4 and 5, c is the concentration of NaPB in solution, $c_{H_2O_2}$ and c_{NaPB} are the concentrations of H_2O_2 and NaPB in the feed streams, $F_{H_2O_2}$ is the volumetric flow rate of H_2O_2 , k_v is the volume shape factor, V is the total volume, ε is the fraction of solid free volume, M_{NaPB} in $M_{H_2O_2}$ are the molecular weights of NaPB in H_2O_2 , m_s and ρ_s are the mass and density of solid phase, and R_n is the mass rate of nucleation.

The following kinetic expressions were used to model the sodium perborate system:

(i) Crystal growth:

$$G = \frac{dL}{dt} = \frac{k_s}{3k_v \rho_s} k_g \eta_r (c - c^*)^g \quad (6)$$

where k_g and g are the growth rate coefficient and growth rate order, k_s is the surface shape factor and η_r is the effectiveness factor.¹⁰ To be able to incorporate the effectiveness factor, one must know the value of the mass transfer coefficient. The values, which were determined by Chianese and coworkers⁶ were taken into account in this work.

(ii) Nucleation

$$B_{u,1} = \frac{\varepsilon}{k_v \rho_s \bar{L}_1^3} \cdot R_n = \frac{\varepsilon}{k_v \rho_s \bar{L}_1^3} k_n \Delta c^n ; \quad \bar{L}_1 = 1 \mu\text{m} \quad (7)$$

(iii) Agglomeration¹⁴

$$R_{a,i} = N_{i-1} \sum_{j=1}^{i-2} 2^{j-i+1} \beta_{i-1,j}(k_a) N_j + \frac{1}{2} \beta_{i-1,i-1}(k_a) N_{i-1}^2 - N_i \sum_{j=1}^{i-1} 2^{j-i} \beta_{i,j}(k_a) N_j - N_i \sum_{j=1}^{\infty} \beta_{i,j}(k_a) N_j \quad (8)$$

where $\beta_{i,j}$ is the agglomeration kernel, a function of the parameter k_a and system supersaturation. Here, we assume that the agglomeration kernel is equal to the product of both.

The population balance based model can be used in two different ways; to solve *forward* or *inverse* problems. While the first approach can be used to predict the process behaviour at different conditions, the second one is solved to estimate unknown kinetics.

Model identification

The estimation of the kinetic parameters from given experimental crystal size distributions requires the solution of the inverse problem. As discussed in the work of Livk *et al.*¹⁵ the crystallisation kinetics can be identified using two approaches: *differential* and *integral*. In the differential approach, the model equations only need to be evaluated at different time instants, while the integral approach requires the integration of the model equations. In this work, a hybrid approach, which combines both methods, is applied.¹⁶ In this way we can make use of our experimental CSDs,

which were obtained by sieving. More details on the experimental procedure are given in the work of Pohar and Livk¹⁷ and Livk et al.⁷ The hybrid approach can be illustrated by the following main steps:

- estimation of the growth rate parameters using the differential method
- estimation of the nucleation and agglomeration parameters using nonlinear optimization together with the values of the growth rate parameters
- iterate the first two steps until a satisfactory agreement between the prediction and experiment is achieved.

The hybrid approach enables a rapid determination of the growth parameters by the differential method in the first step, resulting in a smaller dimensional problem in the second step. The nucleation and agglomeration parameters are estimated in the second step using nonlinear optimization.¹⁸ The nonlinear optimization problem can be written in short as¹⁹

$$\begin{aligned} & \min_{\boldsymbol{\theta}} \Phi(\mathbf{y}^{\text{exp}}(t), \mathbf{y}(t, \boldsymbol{\theta})) \\ & \boldsymbol{\theta} \\ & \text{subject to Crystallization Model} \end{aligned}$$

In the optimization procedure, the value of the parameter set $\boldsymbol{\theta}$, which minimizes the objective function Φ , is estimated. The set of process variables, \mathbf{y} , can contain any suitable process information. However, it is worth noting that the choice of this variable crucially affects the uncertainties of the estimates. The least squares objective function, which includes the number of particles in individual size intervals can be stated as

$$\Phi(\boldsymbol{\theta}) = \sum_{i=1}^{\tilde{m}} \sum_{k=1}^s (N_{k,i}^{\text{exp}} - N_{k,i}(\boldsymbol{\theta}))^2 \quad (9)$$

In the evaluation of the above objective function, only the size intervals obtained by sieving were taken into account. It is also assumed that all the variables in Eq. 9 have the same variance. The complete set of kinetic parameters (Eqs. 6-8) is given as

$$\boldsymbol{\theta}^T = [k_n \quad n \quad k_g \quad g \quad k_a] \quad (10)$$

Using the estimation procedure as explained above, the following values of the parameters were obtained

$$\theta = \begin{bmatrix} k_n \cdot 10^{10} \\ n \\ k_g \cdot 10^6 \\ g \\ k_a \cdot 10^{15} \end{bmatrix} = \begin{bmatrix} 2.768 \\ 4.741 \\ 4.812 \\ 1.086 \\ 0.595 \end{bmatrix}$$

The agreement between the model and experiment is illustrated in Figure 1, where the time evolutions of crystal masses in selected size intervals are presented. Not surprisingly, the agreement is best in the larger size intervals.

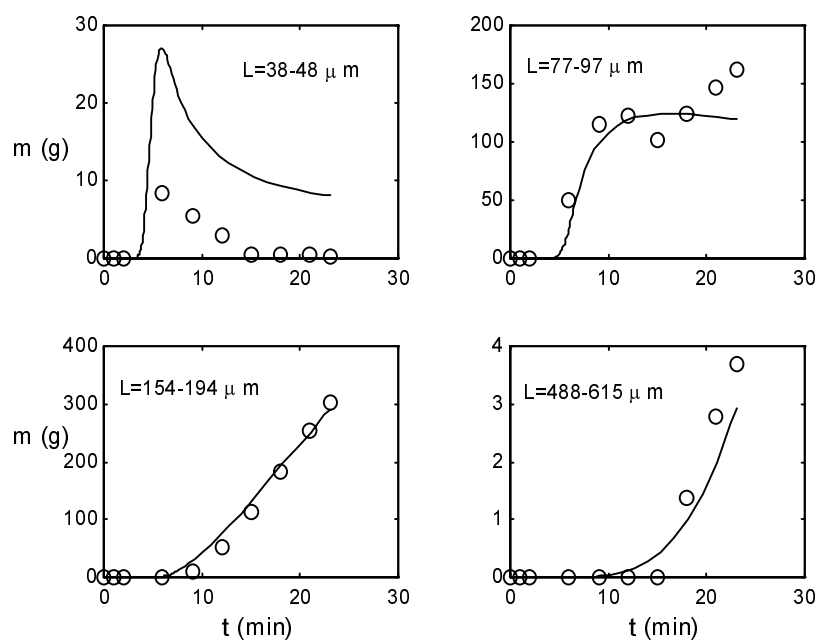


Figure 1. Evolution of crystal masses of various sizes: (o) experiment, (-) model.

Comparison of the estimated kinetics

The sodium perborate precipitation kinetics that are available in the open literature are typically determined at different operating conditions; different degree of mixing and temperature. Keeping this in mind, we only attempt to compare the relative magnitudes

of the kinetics obtained by different authors. In order to simplify the comparison, we transform the linear growth rate from Eq.6, assuming the unity effectiveness factor, into a mass based growth rate²⁰

$$R_g = 4.812 \cdot 10^{-6} \Delta c^{1.086} \quad (11)$$

In Table 1 the growth rates determined by different authors are compared. A mass based equation for the nucleation rate obtained in this work is given as

$$R_n = 2.768 \cdot 10^{-10} \Delta c^{4.741} \quad (12)$$

The values of the nucleation rates obtained by various authors are presented in Table 2.

Table 1. Deposition rates determined by different authors.

	R_g (kg m ⁻² s ⁻¹)	Δc (kg m ⁻³)
Chianese <i>et al.</i> ⁶	$1.35 \cdot 10^{-4}$	20
Chianese <i>et al.</i> ⁵	$2.02 \cdot 10^{-4}$	20
Equation 11	$1.25 \cdot 10^{-4}$	20

Table 2. Nucleation rates determined by different authors.

	R_n (kg m ⁻³ s ⁻¹)	Δc (kg m ⁻³)
Dugua and Simon ⁸	$1 \cdot 10^{-9}$	10
Chianese <i>et al.</i> ³	$5.1 \cdot 10^{-4}$	10
Equation 12	$1.5 \cdot 10^{-5}$	10

The formulation of the agglomeration rate used in the study of David and Bossoutrot⁹ does not enable a comparison of both agglomeration kernels. However, the values of around 10^{-15} , obtained for β in this work, are of the same order of magnitude as the values that were determined for the calcium oxalate system by Collier and Hounslow.²²

Conclusions

The precipitation model development and identification of kinetic parameters for the sodium perborate precipitation is presented in this work. A new approach, which combines the differential and integral methods, has been introduced to estimate the precipitation kinetics. The value obtained for the crystal growth rate is in a good agreement with the values determined by other authors. However, comparing the nucleation rates of different authors a considerable disagreement is found. It would be difficult to judge which of the kinetics, presented in this article, are better suited for the purpose of the design of crystallizers. Nevertheless, the approach presented here can easily be modified to incorporate a higher level of complexity, which may be required in practice.

Nomenclature

B_u	source rate, $\text{m}^{-3}\text{s}^{-1}$
G	linear growth rate, m s^{-1}
g	growth rate order
k_a	agglomeration rate coefficient, $\text{m}^6\text{kg}^{-1}\text{s}^{-1}$
k_g	growth rate coefficient, $\text{kg}^{1-g}\text{m}^{3g-2}\text{s}^{-1}$
k_n	nucleation rate coefficient, $\text{kg}^{-n}\text{m}^{3n-3}\text{s}^{-1}$
\bar{L}_i	characteristic crystal size in the i th size interval
\tilde{m}	number of experimental size intervals
m_s	mass of crystals, kg
N	number of crystals
R_a	agglomeration rate, m^4s^{-1}
R_g	mass deposition rate defined as $1/A dm_s/dt$, $\text{kg m}^{-2}\text{s}^{-1}$
R_n	nucleation rate, $\text{kg m}^{-3}\text{s}^{-1}$
s	number of time instants
t	time

Greek Letters

β	agglomeration kernel, m^3s^{-1}
Δc	supersaturation, kg m^{-3}

References

1. G.Y. Yüksel, S. Titiz, and A. N. Bulutcu, *J. Chem. Eng. Data* **1996**, *41*, 586-588.
2. I. Livk, M. Smodiš, J. Golob, and C. Pohar, *12th Symp. Ind. Cryst.*, **1993**.
3. A. Chianese, A. Contaldi, and B. Mazzarotta, *J. Crystal Growth*, **1986**, *78*, 279-290.
4. O. Söhnle, M. Bravi, A. Chianese, and B. Mazzarotta, *J. Crystal Growth*, **1996**, *160*, 355-360.
5. A. Chianese, *J. Cryst. Growth*, **1988**, *91*, 39.
6. A. Chianese, A. Condo and B. Mazzarotta, *J. Cryst. Growth*, **1989**, *97*, 375.
7. I. Livk, M. Smodiš, J. Golob and C. Pohar, *Cryst. Res. Technol.*, **1995**, *30*(7), 911-920.
8. J. Dugua and B. Simon, *J. Cryst. Growth*, **1978**, *44*, 265-279.
9. R. David and J. M. Bossoutrot, *Chem. Eng. Sci.*, **1996**, *51*(21), 4939-4947.
10. J. Garside, *Chem. Eng. Sci.*, **1985**, *40*(1), 3-26.
11. A.D. Randolph and M.A. Larson, *Theory of Particulate Processes*; 2nd ed., Academic Press, New York, 1988.
12. J.B. Rawlings, S.M. Miller and W.R. Witkowski, *Ind. Eng. Chem. Res.*, **1993**, *32*, 1275-1296.
13. P. Marchal, R. David, J.P. Klein and J. Villiermaux, *Chem. Eng. Sci.*, **1988**, *43*(1), 59-67.
14. M.J. Hounslow, R.L. Ryall and V.R. Marshall, *AIChE J.* **1988**, *34*(11), 1821-1832.
15. I. Livk, C. Pohar and D. Ilievski, *AIChE J.* **1999**, *45*(7), 1593-1596.
16. I. Livk, Disertacija, Univerza v Ljubljani, Ljubljana, 1997.
17. C. Pohar and I. Livk, *Acta Chim. Slov.*, **1997**, *44*(2), 149-159.
18. T.F. Edgar and D.M. Himmelblau, *Optimization of Chemical Processes*; McGraw-Hill, New York, 1988.
19. S.M. Miller and J.B. Rawlings, *AIChE J.*, **1994**, *40*(8), 1312-1327.
20. J.W. Mullin, *Crystallization*, 3rd ed.; Butterworth-Heinemann, Oxford, 1993.
21. A.P. Collier and M.J. Hounslow, *AIChE J.*, **1999**, *45*(11), 2298-2305.

Povzetek

V tem delu obravnavamo dinamično modeliranje kristalizacije iz raztopin. Razvili smo model precipitacije natrijevega perborata, ki napoveduje potek procesa in porazdelitev velikosti delcev produkta. Kinetične parametre hitrosti nukleacije, rasti kristalov in aglomeracije smo izračunali s pomočjo originalne metode, ki združuje lastnosti diferencialne in integralne tehnike. Izračunane vrednosti hitrosti rasti se zelo dobro ujemajo z vrednostmi, ki so jih določili drugi avtorji.